STATISTICS OF CHARGED SOLITONS AND FORMATION OF STRIPES

S. Teber[1], B. P. Stojkovic[2], S. A. Brazovskii[1], A. R. Bishop[2]
[1] *Laboratoire de Physique Theorique et Modeles Statistiques, Bat. 100, Universite Paris-Sud, 91406, Orsay-Cedex, France*
[2] *Theoretical Division and Center for Nonlinear Studies, Los Alamos National Laboratory, Los Alamos, NM 87545*

The $M-$fold degeneracy of the ground state of a quasi-one dimensional system allows it to support topological excitations such as solitons. We study the combined effects of Coulomb interactions and confinement due to interchain coupling on the statistics and thermodynamics of such defects. We concentrate on a two-dimensional case with $M = 2$ which may correspond to monolayers of doped polyacetylene-type polymers or other charge density waves and to junctions in field effect experiments for equivalent materials. Combining analytical and numerical methods, the theory is developed by a mapping to the 2−dimensional Ising model with long range 4-spin interactions. We obtain the phase diagram depending on the ratio of Coulomb interaction and interchain coupling with respect to temperature. The latter exhibits deconfined phases for liquids and Wigner crystals of kinks, and confined ones for bikinks. Also we find aggregated phases with either infinite domain walls of kinks or finite rods of bikinks. Roughening effects due to both temperature and Coulomb repulsion are observed. Applications may concern the melting of stripes in doped correlated materials.

I. INTRODUCTION

Charged interfaces, from their microscopic origin to their macroscopic statistical properties, appear naturally in the study of doped correlated insulators. The latter are characterized by discrete symmetry broken phases with M-fold degenerate ground states, $M > 1$. The interfaces, which are topological configurations whether charged or not, provide a connection between the different ground states. In this framework, quasi-one-dimensional systems, e.g. systems of weakly bound chains, exhibit them at a microscopic level via solitons which emerge as single particles, the $\varphi-$particles[1,2]. This name is related to the fact that each particle provides a phase jump $\varphi = 2\pi/M$, connecting two different but equivalent ground states, within a chain. Their presence therefore breaks the coherence between neighboring chains which must have the same phase modulo 2π. Actually they may exist in a broader range of materials even though their individual detection might be difficult. In this respect, π defects, i.e. $M = 2$, may be interpreted as the building blocks of the experimentally observed stripes in manganite[3] and cuprate[4,5] oxides as well as of the domain walls observed in uniaxial ferroelectric systems[6]. The latter references,[5] and[6], should also provide informations about the charge carried by kinks via measurements of the tilt angle of the stripes and the dipole momentum, respectively.

In one dimension (D) or above the transition temperature, uncharged $\varphi-$particles are allowed to exist as a gas of elementary excitations. They can be defined as strings of reversed spins which, in $D > 1$, cost an energy proportional to their length because of interchain coupling. Below the transition temperature T_c, in the ordered broken symmetry phase, a single soliton would cost infinite energy. The condition for their preservation lies in the concept of *confinement*[7], which limits the string's length leading to finite energy excitations. T_c is thus called the confinement - deconfinement transition temperature. Below T_c, a constant force is originated by confinement which binds the kinks into trains of M particles, to recover the total increment of 2π, within each chain. Going to zero temperature, confinement leads to the aggregation of the trains of solitons belonging to different chains. Thus, the microscopic defects become mesoscopic complexes which span the whole sample at $T = 0$ and can be viewed as domain lines or walls whether the system is, respectively, $2D$ or $3D$[8].

These qualitative arguments strictly apply when solitons are uncharged and must be extended to the case where long ranged Coulomb interactions are present. Indeed, doping correlated insulators leads to the formation of charged topological defects[9]. Also, field effect experiments[10] provide junctions of mobile charged kinks interacting with their images.

The present work deals exclusively with a 2-fold degenerate ground state which corresponds, for quasi-one-dimensional systems, to the well known case of polyacetylene, cf.[9,11,12]. In such ($M = 2$) systems the elementary defects are the $\pm\pi$-solitons. The kink (+) shifts the phase of the CDW from 0 to π while the anti-kink (−) shifts it from π to 2π. Both amplitude-solitons have the same electric charge. The anti-kink of opposite charge, corresponding to the π to 0 shift, is not thermally activated. For the sake of clarity we thus attribute to the $-\pi$-soliton the same graphical representation as the former in Fig. 1. The trains of kinks are then simply pairs of kink−anti-kinks or "bikinks" and the domain lines perpendicular to the chains are formed by such bikinks. We shall examine the statistical properties of kinks under the combined action of the attractive confinement force and the repulsive $3D$ Coulomb force with the help of both analytical and numerical methods.

The paper is organized as follows. In chapter II we present the general model of confinement based on the mapping of a system of interacting kinks to the anisotropic Ising model. In chapter III the phase diagram of the $2D$ system, with competing Coulomb interactions and interchain coupling, is given. Analytically, the results are obtained by various estimates in the case of strong correlations and with the help of a phenomenological model, equivalent to the Ising model below T_c, which has been extended to include weak Coulomb interactions. The thermal roughening of uncharged domain lines, as well as the $T = 0$ Coulomb roughening, are also considered. In chapter IV, numerical simulations are presented. Various regimes of the estimated phase diagram are discussed. The impact of discreteness imposed by numerical simulations is also considered. Details of calculations are given in the Appendix.

II. THE GENERAL MODEL OF CONFINEMENT

We shall follow the method of[13], where the statistics of uncharged kinks in a system of weakly bound chains was studied by *mapping to the Ising model*.

The original Hamiltonian describing the kinks reads

$$\widetilde{H_0} = H_0 - \mu N_s = \int_0^L dx\{- \sum_{<\alpha,\beta>} V\eta_\alpha(x)\eta_\beta(x) + \sum_\alpha (E_s - \mu_s)c_\alpha(x)\}, \tag{1}$$

where N_s is the total number of kinks, E_s is the energy of an isolated kink, μ_s and $c_\alpha(x)$ are, respectively, their chemical potential and local concentration. V is the interchain coupling constant, chosen to be positive. $\eta_\alpha(x)$ is the order parameter describing a kink along chain α.
On the atomic scale a_{0x}, the kink extends over a core length $\xi_0 > a_{0x}$, e.g. $\xi_0 \approx 7a_{0x}$ for polyacetylene, around position x. For this system, the microscopic, domain-wall like, excitation takes the values $\eta = \pm 1$ between the kinks and far from their cores.
The mapping to the two-dimensional Ising model, whose Z_2 symmetry is clearly compatible with the $2-$fold degeneracy of our system, is then based on a coarse graining procedure by introducing a new length scale $a_x > \xi_0 > a_{0x}$, which corresponds to the optimal width of a pair of kinks within a chain under the combined action of interchain interaction and exponential intrachain repulsion between them, cf. Fig. 1. We then discretize the system by $x \to x_n = na_x$ and $y \to y_\alpha = \alpha a_y$ where a_y is the interchain distance. On this scale the order parameter can be restricted to the values ± 1 so it is written as an Ising spin, $S_{n,\alpha}$. The kink density, corresponding to the number of kinks per site, can also be expressed in terms of the Ising spins in the following way. The kink, on chain α for example, is defined *between* two consecutive opposite spins, say on sites n and $n+1$, cf. Fig. 1. The dimensionless density of solitons $\rho_{n,\alpha}$ is related to their dimensional concentration $c_\alpha(x)$, cf. (1), by

$$c_\alpha(x)a_x = \rho_{n,\alpha}. \tag{2}$$

In terms of spins these considerations yield

$$\rho_{n,\alpha} = \frac{1}{2}(1 - S_{n,\alpha}S_{n+1,\alpha}). \tag{3}$$

We see that $\rho_{n,\alpha}$ is unity when a kink is present and zero otherwise.

Introducing these new variables in the first Hamiltonian (1) and including Coulomb interactions we recover the two-dimensional Ising model

$$\widetilde{H} = \widetilde{H_0} + H_c = -J_\perp \sum_{<\alpha,\beta>n} S_{n,\alpha}S_{n,\beta} - J_\parallel \sum_{\alpha,n}(S_{n,\alpha}S_{n+1,\alpha} - 1) + H_{Coul}, \tag{4}$$

where

$$J_\perp = Va_x = K_\perp T \qquad J_\parallel = \frac{1}{2}(E_s - \mu_s) = K_\parallel T. \tag{5}$$

The first term in (4) describes the interchain interaction, responsible for the confinement of the kinks, whose strength is given by the dimensionless coupling constant $K_\perp$. In the second term, $K_\parallel$ is the effective chemical potential of a kink, which has been included as a coupling constant. We emphasize the fact that the energy of a free soliton E_s is always larger than the temperature, so that none of them is thermally activated. We only consider redistributions of the kinks, no matter how they have been created (doping, charge transfer, incommensurabilities), under the combined action of confinement and Coulomb interactions. The latter has been introduced in (4) through

$$H_{Coul} = \frac{e^2}{2\epsilon} \sum_{n,m;\alpha,\beta} \frac{(\rho_{n,\alpha} - \nu)(\rho_{m,\beta} - \nu)}{|\overrightarrow{r}_{n,\alpha} - \overrightarrow{r}_{m,\beta}|}, \tag{6}$$

where $\overrightarrow{r}_{n,\alpha} = (na_x, \alpha a_y)$, $\nu = \overline{c_\alpha(x)} a_x$ is the average dimensionless density of kinks, see (7) below, and ϵ the dielectric constant of the isotropic, neutral media in which the plane is embedded. The Coulomb interaction as written above takes into account the presence of a homogeneous, negatively charged, background of density ν which ensures the electroneutrality of the whole system. It gives the total electrostatic energy of the kinks and the background they are interacting with. The case of dipoles, produced in field effect junctions will be considered later.

As we are working in the grand-canonical ensemble, the key for finding the thermodynamic properties of the system, is to determine the chemical potential of the kinks via the average density per site of kinks:

$$\nu = \frac{1}{2}(1 - < S_{n,\alpha} S_{n+1,\alpha} >) \equiv \frac{1}{2}\left(1 + \frac{1}{T}\frac{\partial f_I}{\partial K_\parallel}\right) \equiv -\frac{\partial \Omega_s}{\partial \mu_s}, \tag{7}$$

where the averaging $< . >$ and the free energy f_I are defined for the ensemble of Ising spins and Ω_s is the grand potential of the solitons, cf.[13].

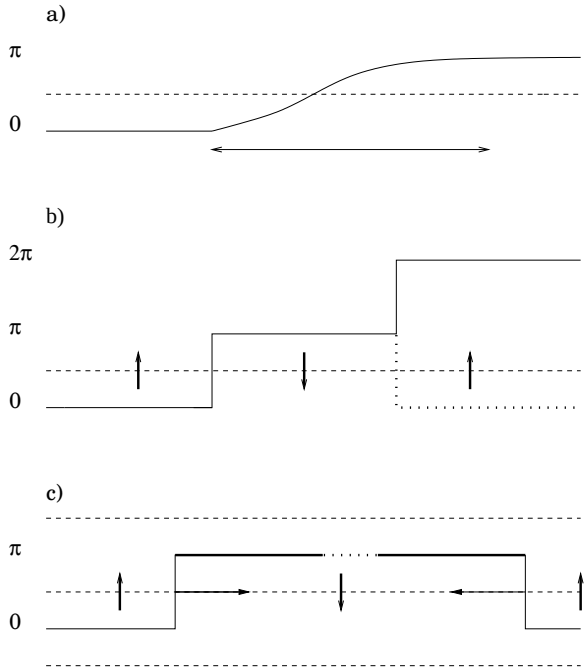

FIG. 1. Figure a) displays a $\pi-$soliton (solid line) along a chain (broken line). The arrow indicates the width ξ_0 of the defect. Figure b) displays the soliton and the antisoliton which correspond to strings of inverted Ising spins after coarse graining. The anti-soliton corresponding to a shift of the phase from π to 2π has the same charge as the soliton. The other anti-soliton (dotted line) has an opposite charge and is not thermally activated.
Figure c) displays a soliton and an antisoliton of the same charge. For simplicity the π to 2π kink has been represented as the π to 0 one which does not exist in our case. Neighboring chains (broken lines) are supposed to be free from defects. Due to interchain interactions (bold lines) the energy of the bikink increases linearly with its size. As a consequence, a constant confinement force binds the solitons. Exponential core repulsion prevents them from annihilating.

III. THE TWO-DIMENSIONAL SYSTEM

A. The dimensionless parameters of the phase diagram

Without Coulomb interaction, the Ising model mapping allows for a complete analysis of the $2D$ case. The aggregation of kinks is controlled by the temperature or the reduced temperature used in the phase diagram,

$$\Theta = \frac{T}{J_\perp}.$$

If their density is weak enough, which we will suppose in the following, below the confinement transition temperature

$$T_c \approx \frac{J_\perp}{\nu} \qquad , \qquad \Theta_c \approx \frac{1}{\nu} \tag{8}$$

the growing confinement energy binds the kinks in pairs with remaining energy $J_\perp$. When the bikinks on neighboring chains stick together below the crossover temperature,

$$T_0 \approx \frac{4J_\perp}{\log(2\nu)} \qquad , \qquad \Theta_0 \approx \frac{4}{\log(2\nu)}, \tag{9}$$

the energy $J_\perp$ is released which results in an adhesion process leading to growing rods. The latter are double lines formed by aggregated bikinks, perpendicular to the chains. Their growth when temperature is further decreased can be seen from the density of solitons and the average rod length $l_\perp$

$$\nu = \frac{\exp(-4K_\perp)}{8K_\parallel^2} \qquad\qquad l_\perp = \frac{a_y}{2K_\parallel} = a_y\sqrt{2\nu}\exp(2K_\perp). \tag{10}$$

These expressions, obtained from the exact solution of the non-interacting Ising model[13] show that as $T \to 0$ the length of the aggregates grows exponentially with temperature until they cross the whole sample more like a system of free domain lines.

On the other hand, the strength of the Coulomb interaction can be characterized by

$$\Gamma = \frac{w_y}{J_\perp} \qquad\qquad w_y = \frac{(ze)^2}{\epsilon a_y} \tag{11}$$

where $s = a_x a_y$ is the unit area of the coarse grained lattice and $z < 1$ takes into account possible fractional charges[9] which may be measured in ferroelectric experiments[6]. Parameters $J_\perp$and w_y give, respectively, the scale of the confinement energy and of the Coulomb energy perpendicular to the chains. They are invariant under coarse graining, thus Γ is also invariant. Unless ϵ is very large the w_y scale is larger than other ones. For example, it is much larger than the energy per particle of a Wigner crystal, which is of the order of $e^2/\epsilon R$ where $R \gg a_{x,y}$ is the mean distance between particles of the Wigner crystal. It is also important with respect to the confinement. In Rydbergs, $1Ry = e^2/\epsilon a_0$, where a_0 is Bohr's radius, we have $w_y = za_0Ry/\epsilon a_y$. In the same units, $J_\perp \approx \nu T_c \approx \nu 10^{-3} Ry$ if we choose $T_c \approx 100K$. Thus for $a_y = 5a_0$ and $\nu = 1\%$ we have

$$\Gamma = \frac{w_y}{J_\perp} \approx z10^2/\epsilon. \tag{12}$$

Taking $z = 1$, the dielectric constant needs to be of the order of 10^2 for the confinement energy to be of the order of the Coulomb energy. This is large but may not be excluded for $\epsilon \sim (\omega_p/\Delta)^2$, where the plasma frequency $\omega_p \approx 10^{-1} - 10$ eV and the gap $\Delta \approx 10^{-2} - 10^0$ eV.
At low temperatures Γ controls the aggregation of the defects in a way similar to Θ at high temperatures. This follows from the derivation of the optimal width x_{opt} of a bikink under the combined action of Coulomb force $e^2/\epsilon x^2$ and the confinement force $-V$:

$$x_{opt} = \sqrt{s\Gamma} \tag{13}$$

This relation holds in all bikink phases whether they are liquid or of the Wigner crystal type. In both phases the average distance between bikinks is given by $R = \sqrt{s/\nu}$. As long as $x_{opt} \ll R$ the elongation x_{opt} can be neglected so that, in zero approximation, the bikink can be considered as a well defined particle of charge $2e$. On the other hand when x_{opt} is of the order of R, bikinks deconfine and the system consists of interacting solitons. These remarks are weakly modified at non zero temperature as long as $\Theta \ll 1$. This follows from the fact that thermal fluctuations shift the mean width of the bikink to $\overline{x} \approx x_{opt} + a_x\Gamma^{1/4}\Theta^{1/2}$. Thermal fluctuations can be neglected as soon as $\Gamma \gg \Theta^2$. Unless ϵ is large, cf. (12), this condition is well satisfied below Θ_0.

B. Wigner crystals of kinks and bikinks

Below Θ_0, when the condition $\Gamma \gg \Theta^2$ is satisfied, bikinks order in the form of a Wigner crystal. The ratio $x_{tot}/R = \sqrt{\Gamma\nu}$ is another control parameter which defines a crossover to a deconfined phase consisting of a Wigner crystal of solitons. The Lindeman criterion specifies that the crossover occurs when the mean square deviation of the width x_{opt} becomes of the order of a fraction of R. With the small Lindeman number γ the transition is thus expected at

$$\Gamma_c \sim \gamma/\nu, \tag{14}$$

which scales as Θ_c.
This deconfinement transition with respect to the bikinks can be easily derived from the Wigner crystal phase of solitons. The energy per particle of the Wigner crystal of solitons is $-e^2/\epsilon R$ and the confinement energy $\sim J_\perp R/a_y$. A confinement crossover, with respect to the solitons, takes place when both energies are of the same order. Taking into account the Lindeman number, we recover (14).
These results are summarized in the phase diagram of figure 3.

C. The interacting rod phase

The Coulomb interactions are expected to be especially important for aggregated phases, e.g. rods and lines, because of the size-dependent charging energy cost of the aggregation,

$$\Sigma(n) \approx 2w_y n \log(\frac{min(na_y, l_D)}{a_x}), \tag{15}$$

where n is the number of solitons belonging to each of the two lines formed by the rods and l_D is the Debye screening length. The latter is determined by the density response function $\partial\nu/\partial\mu_s$ which, for the $2D$ plane embedded in $3D$ space, is

$$\frac{1}{l_D} = \frac{2\pi e^2}{\epsilon s}\frac{\partial\nu}{\partial\mu_s}. \tag{16}$$

We shall consider the case of relatively weak Coulomb interactions which does not prevent the actual existence of the aggregates while affecting their statistical properties. The required condition is that $\Gamma \ll 1$. Our aim is then to formulate the general expressions which yield the density of kinks and their mean length. This can be done with the help of a phenomenological model which has been shown to adequately reproduce the results of the exact solution[13]. The rods can fuse into longer ones or disintegrate into shorter ones, equilibrating their chemical potentials. The main effect of the Coulomb interaction is to shift the energy $E(n)$ of each aggregate of length na_y by its self-energy (15) while preserving their shapes. The free energy of the system is then

$$f_{rod} = \sum_{n=1}^{\infty} \left(c(n)E(n) + Tc(n)\log(c(n)/e)\right), \tag{17}$$

where $c(n)$ is the density of rods of length na_y, the second term is the entropy of the Boltzmann-like rod gas, and

$$E(n) = 4J_\perp + 2E_s n + \Sigma(n) \tag{18}$$

is the energy of a rod of length na_y. The first term in (18) corresponds to the confinement energy paid by the tips of the rod. In the second term we have taken into account the fact that there are two kinks per unit length of the aggregate.
Minimizing the free-energy with the constraint that the total number of particles is constant,

$$0 = \frac{\partial}{\partial c(n)}\left(f_{rod} - \mu_s \sum_l 2nc(n)\right), \tag{19}$$

the density of kinks is then given by

$$\nu = \sum_{n=1}^{\infty} 2nc(n) = e^{-4K_\perp} \sum_{n=1}^{\infty} 2n \exp\left(-4nK_\parallel - \beta\Sigma(n)\right), \tag{20}$$

where $K_\parallel$ is related to the chemical potential of the solitons μ_s by (5). Thus, expression (20) allows one to fix μ_s. Finally, the average length of the domain line reads

$$l_\perp = a_y \frac{\nu}{c} \qquad\qquad c = \sum_{n=1}^{\infty} c(n). \tag{21}$$

From (20) and (21) with $\Sigma(n) \equiv 0$ we recover the results in (10). As will be shown in subsequent paragraphs, screening by normal carriers, cf. l_D, is important in the present regime. Self-screening in the ensemble of solitons is also considered. It plays a dominant role at $T = 0$, especially for stronger Coulomb interactions corresponding to $\Gamma \gg 1$.

1. The case of efficient screening

The efficiency of the bulk screening is manifested by the fact that the Debye length l_D is shorter than the average length of the domain line $l_\perp$. Considering a distribution of rods with lengths $na_y > l_D$, we arrive, with the help of (15) and (20), at the expressions given in (10) with $K_\parallel \to K_\parallel^*$, where

$$K_\parallel^* = K_\parallel + \frac{1}{2T} w_y \log(\frac{l_D}{a_x}) \tag{22}$$

is the effective chemical potential shifted by the Coulomb self-energy. We can now check our original hypothesis $l_\perp > l_D$. We have with the help of (16)

$$l_D^{-1} = \frac{2\pi e^2}{\epsilon s} \frac{\exp(-4K_\perp)}{T} \frac{1}{(2K_\parallel^*)^3}. \tag{23}$$

Thus

$$\frac{l_\perp}{l_D} \approx \frac{2\pi e^2}{a_x} \frac{\exp(4K_\perp)}{T} (2\nu)^2,$$

which grows as $T \to 0$, i.e. $l_\perp / l_D \to \infty$. Therefore, thanks to the presence of an effective bulk screening, the interacting system can be mapped to the non-interacting one, in the limit $K_\perp \gg 1$, proving the growing macroscopic aggregation of the defects.

2. The case of weak screening

More surprising is the case of *weak* screening which corresponds to $l_\perp < l_D$. Considering a distribution of rods with lengths $na_y < l_D$, (20) then becomes

$$\nu \approx e^{-4K_\perp} \int_0^{l_D} dn 2n \exp\left(-4nK_\parallel - 2n \frac{w_y}{T} \log(\frac{na_y}{a_x})\right) \tag{24}$$

where the second term in the exponent comes from the self-energy of a rod of length n. Due to the non-linearity of the self-energy the chemical potential cannot simply be shifted as in the previous case. Moreover, the Coulomb energy makes the sum converge even for a zero value of the chemical potential. In order to balance the Coulomb interaction and thus keep a given non-zero ν, we must allow $K_\parallel$ to acquire negative values in (24). To show this, we notice that the integral in (24) can be evaluated with the help of a saddle point approximation, which is valid for large, negative $K_\parallel$. At the saddle point the argument of the exponential in (24) has a sharp maximum for

$$l_{sp} \approx \exp\left(\frac{2T|K_\parallel|}{w_y}\right) \tag{25}$$

and (24) becomes

$$\nu \exp(4K_\perp) \approx 2\sqrt{\frac{Tl_{sp}}{w_y}} \exp\left(\frac{w_y}{T} l_{sp}\right). \tag{26}$$

From (16) and (24) at the saddle point, the Debye length reads

$$\frac{1}{l_D} \approx \frac{w_y}{Ta_x} \nu l_{sp}. \tag{27}$$

As we work at constant ν, l_{sp} is given by (26)

$$l_{sp} \approx 4\frac{J_\perp}{w_y} + \frac{T}{w_y} \log\left(\frac{\nu}{4} \frac{w_y}{\sqrt{J_\perp T}}\right). \tag{28}$$

Due to the weak Coulomb interaction $\Gamma \ll 1$ and the sharpness of the saddle point ensured by $w_y \gg T$, the second term in (28) is a correction with respect to the first. The second term is responsible for the increase of l_{sp} with decreasing temperature as long as

$$T > \frac{\nu^2 w_y^2}{16 J_\perp} = T_l. \tag{29}$$

Hence, in this regime, $l_{sp} \approx 4J_\perp/w_y$ and (27) yields

$$\frac{l_{sp}}{l_D} \approx \frac{16 J_\perp^2}{T w_y} \nu. \tag{30}$$

When l_{sp} reaches l_D a crossover from the actual process of growth, involving negative $K_\parallel$, to the previous one will take place at T_{cr} defined, with the help of (30), by

$$\frac{T_{cr}}{T_c} \approx 16\nu^2 \frac{J_\perp}{w_y}, \tag{31}$$

where (8) has been used. From (29) and (31) we have

$$\frac{T_{cr}}{T_l} \approx \frac{16^2}{\nu} \left(\frac{J_\perp}{w_y}\right)^3 \gg 1, \tag{32}$$

where we have also used the fact that we are in the weak Coulomb regime. Thus (32) indicates that the well screened regime ($l_{sp} > l_D$) is reached before temperature is low enough to disfavor the growth of the rods, i.e. (29) is satisfied. We summarize the case of weak screening as follows.

Without Coulomb interactions, the rods started to form at $T < T_0 \approx J_\perp/|\log \nu|$ and then grew exponentially with an activation energy $4J_\perp$; as temperature approached zero, the chemical potential approached zero exponentially, cf. (10).

In the case of weak Coulomb interaction ($w_y < J_\perp$), at low temperatures ($T \ll w_y$) the behavior of the system is very different. Remarkably, negative $K_\parallel$ corresponds to the Ising model with antiferromagnetic coupling along the chains. Nevertheless, 4−spin Coulomb interactions (6) keep the system in the ferromagnetic state so as to preserve electroneutrality. The average length of the aggregates l_{sp} is approximately $J_\perp/w_y$ with weak deviations linear in temperature up to some logarithmic corrections, cf. (28). These deviations lead to an increase of l_{sp} when T decreases. The chemical potential $T|K_\parallel|$ moves down within the negative regime but logarithmically slow as can be seen from (25). Meanwhile the compressibility $\approx \partial\nu/\partial\mu_s$ increases so that the screening length decreases linearly with temperature, cf. (27). At T_{cr} the Coulomb interaction becomes screened. The system then returns to the exponential growth of $l_\perp$ as for the noninteracting system.

3. Application to field effect junctions

To finish with this section we mention that the logarithmically growing self-energy is peculiar to a doped system. In the case of a layer produced by a field effect experiment, dipoles order in lines of length $a_y n$ and the associated energy is

$$E_{dip}(n) = \frac{(ed)^2}{2a_y^2} n \left(\frac{1}{a_x^2} - \frac{1}{(a_y n)^2} \right),$$

where d is the distance between a charge and its image. As we are interested in large n, this energy becomes linear in n. Thus this case is similar to the well screened case.

D. Thermal and Coulomb roughening of domain lines

1. Thermal roughening of lines

The effect of thermal fluctuations on the aggregates of the non-interacting system can be derived from the solid-on-solid (SOS) model which is well known in the field of random interfaces, cf.[14] for more details. In this model a line made of one topological charge, i.e. a domain line, is described by integer-valued height variables x_k $(k = 1, ..., l_\perp)$ which define the position of kinks along the chains with respect to their $T = 0$ position. The energy of an SOS interface at $T \to 0$, i.e. $K_\perp \to \infty$ and $l_\perp \to \infty$, can then be taken as[14]

$$\beta H_{SOS} = 2K_\perp \sum_{k=1}^{l_\perp} |x_k - x_{k-1}|. \tag{33}$$

The difference correlation function is then[14]

$$< (x_k - x_j)^2 >_{SOS} = 2|k-j| \frac{\exp(-2K_\perp)}{1 + 2\exp(-2K_\perp)}. \tag{34}$$

Expression (34) shows that the correlation function diverges in the limit $|k - j| \to \infty$. This is a signature of the *roughening* of the domain line at any non zero temperature. This roughening leads to collisions between different lines separated by a distance a_x/ν. Taking into account the fluctuations of one line, neighboring lines remaining straight for simplicity, a collision takes place once the mean fluctuation in $x-$direction is of the order of a_x/ν. Collisions of lines can be equivalently interpreted as disintegration of rods as can be seen from (34). With $< (x_k - x_j)^2 >_{SOS} \approx 1/\nu^2$, the temperature at which rods of length $l_\perp \approx |k - j|$ are formed is given by

$$T \approx \frac{2J_\perp}{|\log(l_\perp \nu^2)|}. \tag{35}$$

Equation (35) shows that rods reduce to bikinks ($l_\perp \approx 1$) when $T \geq T_0$ in agreement with what has been said in the preceding paragraphs.

2. Coulomb roughening of lines

In previous sections we have shown that the growing of the aggregates as we approach zero temperature is mainly due to an effective bulk screening. However, at $T = 0$ all kinks have aggregated into domain lines which cross the whole sample. Thus, no screening charge remains and no confinement energy, due to interchain interactions, is paid by the lines. The latter implies that two domain lines, each made of one type of topological charge, will be far apart. On the other hand, because there is no more screening charge, the competition between Coulomb interaction and confinement leads to *roughened lines,* as shown below. It is a signature of the *self-screening* of the domain lines. This roughening may be considered separately from the thermal roughening we discussed previously.
First, we give some simple estimates concerning the form of the line. The latter corresponds to a linear distribution of charges and it's equilibrium shape is determined by allowing one of it's constituent kinks to find it's equilibrium position under the combined action of the Coulomb repulsion and the attractive confinement force. The Coulomb force $F_{coul} = w_y/x$ originates from the infinite line and is balanced by the confinement force $F_{conf} = -V$. The optimal equilibrium position of a kink emitted from the line is

$$x_0 \approx \frac{w_y}{J_\perp} a_x = \Gamma a_x. \tag{36}$$

For $\Gamma \gg 1$, the linear distribution acquires a width $x_0 \gg a_x$. This finite width is a manifestation of the self-screening of the rods which leads to their roughening.

A particular distribution of kinks *within* the roughened domain line requires a more elaborate analysis. We consider a general distribution characterized by the variational parameters x_0 and y_0. The latter correspond to the periodicity of the distribution while the former is the modulation amplitude. They are found by minimizing the total energy per chain, E_{tot}, of the distribution. The latter is

$$E_{tot} = E_{coul} + E_{conf} \tag{37}$$

with the Coulomb energy per chain

$$E_{coul} = \frac{w_y}{L}\int_0^L \frac{dydy'}{a_y^2}\frac{1}{\sqrt{(y-y')^2 + (x(y)-x(y'))^2}}, \tag{38}$$

where L is the size of the system in the y direction. The confinement energy per chain is

$$E_{conf} = \frac{a_y}{y_0}\frac{J_\perp}{a_x}\int_0^{y_0} |\frac{dx}{dy}|dy.$$

In the case $x_0 \ll y_0$, (45) in the Appendix and (37) yield in the main logarithmic approximation

$$E_{tot} \approx -2w_y\left(\frac{x_0}{y_0}\right)^2 \log\left(\frac{y_0}{a_x}\right) + 4a_y\frac{J_\perp}{a_x}\frac{x_0}{y_0}. \tag{39}$$

We clearly see from the last expression that the energy is not bounded from below for $x_0 \approx y_0 \to \infty$. The starting hypothesis $x_0 \ll y_0$ is thus not satisfied. In the second case $x_0 \gg y_0$. With the help of (47) in the Appendix, the total energy per chain is

$$E_{tot} \approx -2w_y \log\left(\frac{x_0}{a_x}\right) - 2w_y\frac{y_0}{x_0}\log\left(\frac{x_0}{y_0}\right) + 4a_y\frac{J_\perp}{a_x}\frac{x_0}{y_0}. \tag{40}$$

Minimizing with respect to x_0 and y_0 leads to $x_0 \approx y_0 \to \infty$, again in contradiction with the starting hypothesis $x_0 \gg y_0$.
These contradictions imply that the modulated line minimizes its energy at intermediate values of $r_0 = x_0/y_0$, e.g. $r_0 \approx 1$, where the Coulomb energy is of the order of the confinement energy. In this regime, (37) is difficult to treat analytically.
We thus consider an ansatz giving the distribution of the kinks. Numerical simulations give zig-zag shapes. In this connexion we show in the Appendix that a sinusoidal profile

$$x(y) = x_0 \sin(2\pi\frac{y}{y_0})$$

gives a correct description of the distribution in the continuum limit. The total energy is then given by

$$E_{tot} = \frac{4}{\pi}w_y\int_{a_x/y_0}^{l_D/a_x} dt\frac{1}{\sqrt{t^2 + 16\pi^2 r_0^2\sin^2(t)}}K\left(\frac{4\pi r_0|\sin(t)|}{\sqrt{t^2+16\pi^2r_0^2\sin^2(t)}}\right) + 4a_y\frac{J_\perp}{a_x}r_0, \tag{41}$$

where the upper cut-off corresponds to the dimensionless Debye length and $K(k)$ is the complete Elliptic function of the first kind. The lower cut-off in the $t-$integral gives rise to the asymmetry between x_0 and y_0, which is already present in (39) and (40). As the sinusoidal distribution is valid in the continuum limit we shall take $a_x \to 0$ and $a_y \to 0$ keeping other lengths fixed. (41) then depends only on r_0 . The numerical plot of this energy clearly shows a minimum for $r_0 \approx 1.2$, cf. Fig. 2, which agrees with the analytical predictions.

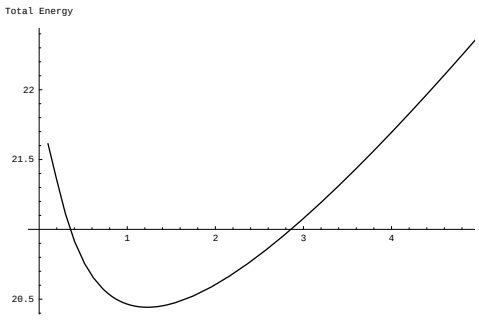

FIG. 2. The total energy (41) with respect to r_0.

With the help of (36) these results lead to

$$x_0 \approx y_0 \approx (w_y/J_\perp)a_x \gg 1. \tag{42}$$

The condition that the lines do not overlap, $x_0 \ll 1/\nu$, returns us to the boundary $\Gamma < \Gamma_c = 1/\nu$ separating the phase of linear aggregates from the Wigner crystal of bikinks.
A tilted stripe, which corresponds to a small argument of the sine distribution above, is easily shown to better minimize the energy. This fact is relevant in the context of cuprate oxides[5].

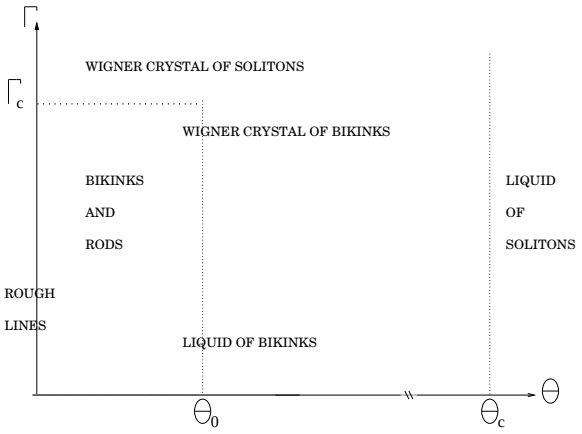

FIG. 3. Phase diagram of the $2D$ model.
Θ_c is the confinement transition temperature below which solitons aggregate into bikinks. Θ_0 is the crossover temperature below which bikinks aggregate into growing rods. At $\Theta = 0$ the latter are roughened domain lines perpendicular to the chains when the Coulomb interaction $\Gamma < \Gamma_c$. For $0 < \Theta < \Theta_0$ this confined phase consists of aggregates screened by a liquid or a Wigner crystal of bikinks, depending on the strength of the Coulomb interaction. When $\Gamma > \Gamma_c$ both the lines at $\Theta = 0$ and the aggregates with their screening charges at $0 < \Theta < \Theta_0$ crossover to a deconfined phase, the Wigner crystal of solitons.

IV. NUMERICAL APPROACH

In this section we consider the results obtained with the help of numerical methods. The calculations have been performed in the canonical ensemble with periodic boundary conditions. The latter implies interaction of each kink, within a computational cell, not only with all other kinks but also with all their images residing in cells obtained by translation from the original computational cell[16]. This results in an effective electrostatic interaction which is periodic in the computational cell used and which can be properly tabularized for rapid evaluations[17]. At the beginning of each simulation we place the kinks at random and assign the sign to all of the Ising variables $S_{n,\alpha}$ accordingly. We study the energy landscape of the system using the classical Monte Carlo technique with the standard Metropolis algorithm for the acceptance of kink motion. In order to rapidly reach configurations with the lowest energy, we perform simulated annealing from high temperatures with a variable sampling time range. We emphasize the common points between these numerics and the various points discussed above. Also, the impact of discreteness within the simulations is considered.

A. The parameters of numerical simulations and the impact of the coarse graining

The typical values taken in numerical simulations are $J_\perp \approx 10^{-1}eV$, $\nu \approx 1\%$ and $a_y \approx 4,5A$. This leads to $\Theta_c \approx 100$, $\Theta_0 \approx 1$, as above, and $\Gamma \approx 10/\epsilon$. The Coulomb interaction is then monitored with the help of the dielectric constant. The value assigned to the coarse graining length needs some more care. It must be at least of the order of the core of a soliton ($\xi_0 \approx 7A$ in polyacetylene). However, if it is too large the ground state of the system may be unreachable because of commensurability effects due to the discreteness of the lattice. The latter are especially relevant in the Wigner crystal phases where a pinning by the lattice occurs which distorts the Wigner crystal from its equilibrium position. We shall therefore estimate the upper boundary, allowing neglect of such commensurability effects, which can be reached by a_x.

We suppose that kinks form a Wigner crystal with their positions $x_{n,\alpha}^{(eq)}$ in equilibrium, i.e. at the lowest energy distribution which is the triangular lattice[15]. This structure melts when the fluctuations u of the kinks around their equilibrium position is a fraction γ, the Lindeman number, of their mean separation $\sqrt{s/\nu}$. The new positions are $x_{n,\alpha} = x_{n,\alpha}^{(eq)} + u$, with $u = \gamma\sqrt{s/\nu}$, $\gamma < 1$. Usually the melting is due to thermal or quantum fluctuations. However, if the coarse graining imposed by simulations is greater than u, kinks will also never reach their equilibrium position and the Wigner crystal will not be observed. Instead a two-dimensional commensurate phase will form. Thus, the coarse grained length must satisfy the condition $a_x < u = \gamma\sqrt{\xi_0 a_y/\nu}$. With the typical values given above this yields $a_x < 50\gamma A$. For this range of the coarse graining length the kinks will be able to adjust themselves and not be influenced by the underlying lattice. Supposing that $\gamma \approx 0,5$ gives an overestimated value of the maximum length, $a_x \approx 25A$.

B. Numerical results

Figure 4 shows the non-interacting phase at temperatures $0 \ll \Theta < \Theta_0$. This phase has been obtained from the interacting case by imposing a large dielectric constant $\epsilon \sim 10^9$ so that $\Gamma \ll 1$. In accordance with what has been said concerning the non-interacting phase, a gas of bikinks is present and the latter aggregates into rods perpendicular to the chains.

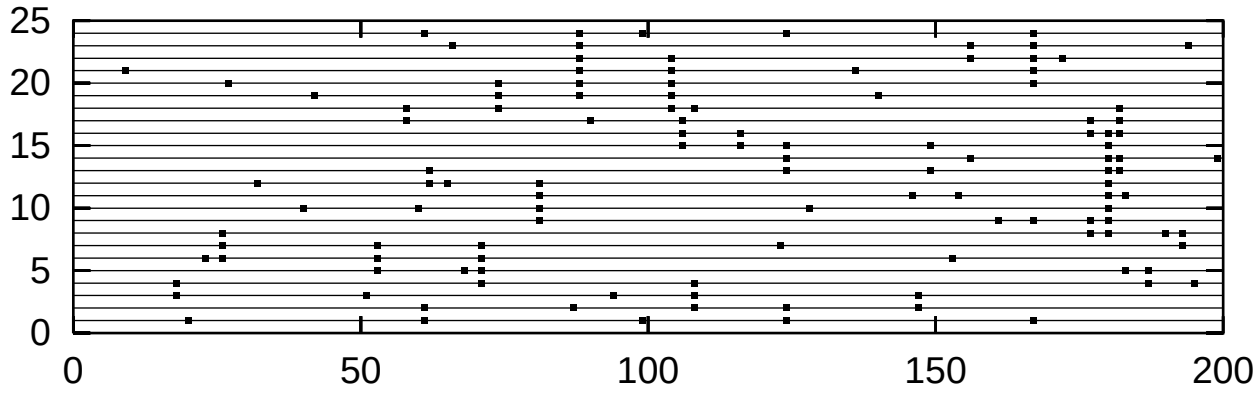

FIG. 4. The non-interacting rod phase corresponding to $0 \ll \Theta < \Theta_0$.
This phase has been obtained by imposing a large dielectric constant. The computational cell displays the chains as horizontal lines, and their excitations as the points. Each excitation corresponds to the presence of a reversed spin with respect to the ferromagnetic ground state and thus represents a bikink. The aggregation of bikinks leads to the presence of rods perpendicular to the chains.

Turning on the Coulomb interactions and adjusting the dielectric constant such that $\Gamma \approx 1 \ll \Gamma_c$, we have at $\Theta = 0$ a one dimensional Wigner crystal of domain lines as shown in figure 5.

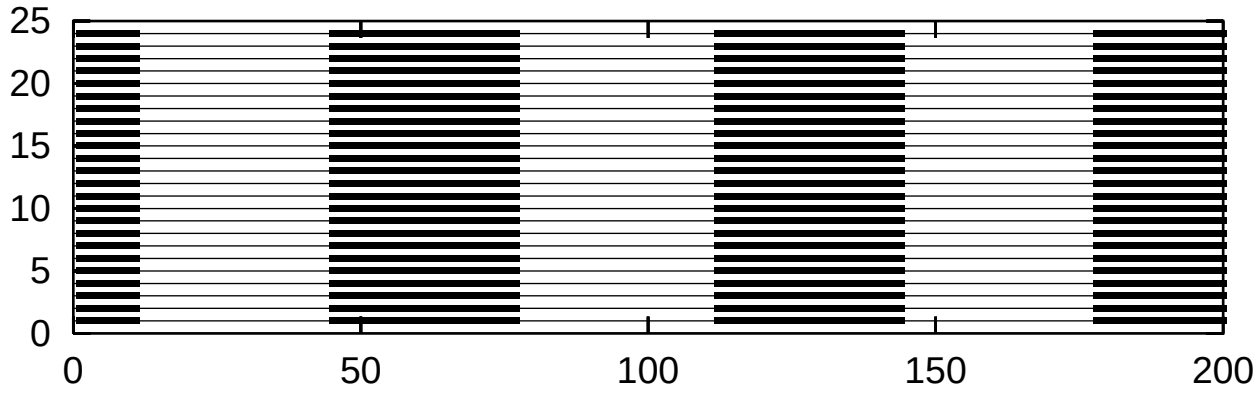

FIG. 5. Domain lines at $\Theta = 0$ for a weak Coulomb interaction $\Gamma \approx 1$.
As temperature approaches zero the rods of figure 4 cross the whole computational cell more like a system of domain lines. In the presence of a weak Coulomb interaction these lines order in the form of a one dimensional Wigner crystal.

Turning on stronger Coulomb interactions the lines acquire a modulated shape in accordance with what has been said in section III C; the result is displayed in Fig. 6 for $\Gamma \approx 10$. By comparison with Fig. 5 the lines are still forming a periodic pattern. They roughen as a result of the competition between Coulomb interactions and confinement.

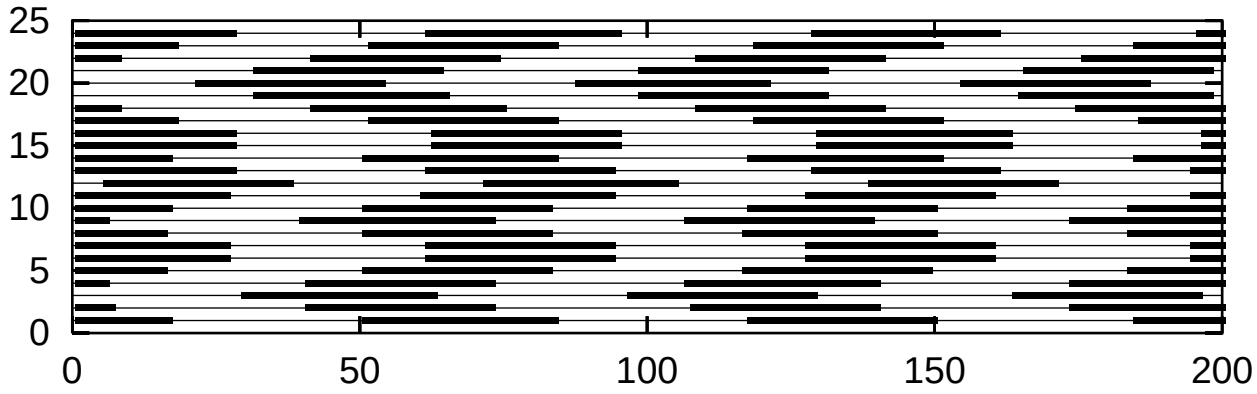

FIG. 6. Modulated domain lines at $\Theta = 0$ and $1 \ll \Gamma < \Gamma_c$
A Coulomb roughening of the domain lines takes place when Coulomb interaction is increased, in agreement with the results of paragraph III C.

V. CONCLUSION

We have considered the effect of two competing long range interactions, Coulomb and confinement, on the thermodynamic properties of systems with two-fold degenerate ground-states. Analytical and numerical methods have been used and compared. The theory has been developed along the lines of the non-interacting case where a mapping to the Ising model allowed for an exact solution in $2D$. Due to the complications brought by the Coulomb interactions, we have studied, in a semi-phenomenological way, the main features which distinguish the present case from the non-interacting one. In $2D$ the main parameter controlling the aggregation of solitons in the presence of the long range interactions is Γ in equation (11), i.e. the ratio between the Coulomb energy scale and the confinement scale. This parameter, below the crossover temperature Θ_0, cf. (9), is analogous to temperature above the confinement transition Θ_c, cf. (8). The various confined and deconfined phases have been displayed on the phase diagram Fig. 3 depending on Γ and temperature. We have concentrated on the low temperature regime , i.e. below Θ_0, where we have shown that a crossover line $\Gamma_c \sim 1/\nu$ separates a confined phase of bikinks and their aggregates from a deconfined phase which is a Wigner crystal of solitons. As expected, in the aggregated phases, e.g. rods and lines, the Coulomb interactions may play a crucial role because of the size dependent charging energy of the solitonic complexes. In the case of weak Coulomb interactions $\Gamma \ll 1$, the efficiency of the bulk screening insures the preservation of the aggregates. The main effect of the long range interactions is to shift the chemical potential of the elementary defects by the Coulomb self-energy (22). However, when bulk screening is no longer efficient, we have found that antiferromagnetic interactions along the chains are necessary in order for the system to adjust the correct density of solitons and conserve the aggregates (24). The ground state of the system remains ferromagnetic to maintain the electroneutrality. In both cases, efficient and weak screening, a growing macroscopic aggregation takes place. Because of thermal roughening, only at $T = 0$ do the complexes of solitons span the whole sample in the form of domain lines (34). We have shown that the latter are stable for larger Coulomb interactions $1 \ll \Gamma < \Gamma_c$ due to self-screening in the ensemble of solitons. This is manifested by the Coulomb roughening of the lines in accordance with numerical results, cf. Fig. 6. The parameters of the distribution were derived from a variational procedure (42). In the continuum limit a sinusoidal profile gives a correct description of the rough lines.

APPENDIX

We consider the periodic modulation for a general distribution of kinks $x(y)$. The Coulomb potential energy associated with this distribution is given by (38). Going to the new variables $t = (y - y')/2$ and $s = (y + y')/2$ expression (38) becomes

$$E_{coul} = \frac{2w_y}{L} \int_{a_x}^{L} ds \int_{a_x}^{L} \frac{dt}{a_y} \left\{ \frac{1}{\sqrt{t^2 + (x(s+t) - x(s-t))^2}} - \frac{1}{t} \right\}. \tag{43}$$

The integral has been regularized by subtracting the infinite contribution coming from the straight line $x(y) \equiv 0$.

In the case where $x_0 \ll y_0$, (43) can be divided as follows:

$$E_{coul} = \frac{2w_y}{L} \int_{a_x}^{L} ds \left[\int_{a_x}^{x_0} + \int_{x_0}^{y_0} + \int_{y_0}^{L} \right] \frac{dt}{a_y} \left\{ \frac{1}{\sqrt{t^2 + (x(s+t) - x(s-t))^2}} - \frac{1}{t} \right\}. \tag{44}$$

In all integrals in (44) we can expand $x(s \pm t) \approx x(s) \pm t x'(s)$. Thus the t and s integrals decouple and we obtain

$$E_{coul} \approx -2w_y \left(\frac{x_0}{y_0} \right)^2 \log \left(\frac{y_0}{a_x} \right). \tag{45}$$

In the opposite case, $x_0 \gg y_0$, we have

$$E_{coul} \approx \frac{2w_y}{L} \int_{a_x}^{L} ds \left[\int_{a_x}^{x_0} + \int_{x_0}^{L} \right] \frac{dt}{a_y} \left\{ \frac{1}{\sqrt{t^2 + (x(s+t) - x(s-t))^2}} - \frac{1}{t} \right\}. \tag{46}$$

In the present case the expansion of $x(s \pm t)$ needs some care because $x_0 \gg y_0$ and the s and t integral do not easily decouple. The first $t-$integral, in (46), is over $x_0/y_0 \gg 1$ periods. Its major contribution is at the vicinity of the zeros of $x(s+t) - x(s-t)$. These zeros exist for any s and correspond to "nesting" points $t_n \equiv n y_0/2$ with $n = 1, 2, ...2r_0$. From these considerations and with the help of $\delta t = t - t_n$, the major contribution to the integral reads

$$2w_y \sum_{n=1}^{2r_0} \int_0^{\frac{y_0}{2}} \frac{d\delta t}{a_y} \frac{1}{\sqrt{t_n^2 + 4\delta t^2 x'^2(s)}} \approx \frac{2w_y}{|x'(s)|} \sum_{n=1}^{2r_0} \log \left(\frac{4x'(s)}{n} \right) \approx -2w_y \int_{\frac{1}{r_0}}^{1} dn \log(n),$$

where $r_0 = x_0/y_0$ and we have taken $x'(s) \approx r_0$. Thus, restricting ourselves to the main logarithmic approximation, we obtain

$$-2w_y \log \left(\frac{x_0}{a_x} \right) - 2w_y \frac{y_0}{x_0} \log \left(\frac{x_0}{y_0} \right).$$

In the second $t-$integral t is large and we can expand the denominator in $x(s+t) - x(s-t)$. Going to the first order in $1/r_0$ the result is compensated by the regularizing term and thus gives zero.
The Coulomb energy then reads

$$E_{coul} \approx -2w_y \frac{y_0}{x_0} \log \left(\frac{x_0}{y_0} \right) - 2w_y \log \left(\frac{x_0}{a_x} \right). \tag{47}$$

The total energy of the system we are considering includes the potential energy and the confinement energy. The latter can be taken, for any x_0, as

$$E_{conf} = a_y \frac{J_\perp}{a_x} \int_0^{y_0} |\frac{dx}{dy}| dy = 4a_y \frac{J_\perp}{a_x} \frac{x_0}{y_0} \tag{48}$$

Combining (48) with either (45) or (47) the total energy per chain is thus given by (37).

A particular function $x(y)$ describing a single domain line in the two-dimensional plane at $T = 0$ can be estimated. As implicitly assumed in (48), the confinement of this aggregate can be taken into account, in the Hamiltonian, with the help of a solid on solid model:

$$H = \frac{1}{2\epsilon} \sum_{y,y'} \frac{e^2}{\sqrt{(x(y) - x(y'))^2 + (y - y')^2}} + V \sum_y |x(y) - x(y - a_y)|. \tag{49}$$

Minimizing (49) with respect to $x(y)$ yields the recurrence relation

$$x(y) = \frac{\kappa^2 \left(sign\left(x(y) - x(y-a_y)\right) - sign\left(x(y+a_y) - x(y)\right)\right) + \sum_{y'} x(y') \left[\left(x(y) - x(y')\right)^2 + \left(y - y'\right)^2\right]^{-3/2}}{\sum_{y'} \left[\left(x(y) - x(y')\right)^2 + \left(y - y'\right)^2\right]^{-3/2}}, \quad (50)$$

where *sign* is the sign function and $\kappa^2 = \epsilon V/e^2 = (\xi_0 a_y \Gamma)^{-1}$, has a unit of inverse length squared and is related to (36). The solution $x(y)$ cannot easily be found analytically. However simulations give us a hint for they show a kind of zig-zag distribution. This suggests using a sinusoidal ansatz

$$x(y) = x_0 \sin(2\pi \frac{y}{y_0}). \quad (51)$$

Comparing the resulting plot of each side of (50) we can check the accuracy of this approximation. The result is displayed in Figure (7), which shows that the sinusoidal distribution is correct in the continuum limit.

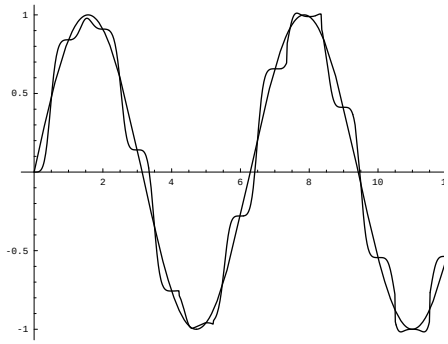

FIG. 7. The sinusoidal distribution.

[1] M. J. Rice, A. R. Bishop, J. A. Krumhansl, S. E. Trullinger, Phys. Rev. Lett. **36** (1976) 432

[2] S. Brazovskii, J. Phys. IV France, **10** (2000), Pr3-169, cond-mat 0006355

[3] S. Mori, C.H. Chen, S.-W. Cheong, *Nature*, **392** (1998) 473

[4] J. M. Tranquada in *Neutron Scattering in Layered Copper-Oxide Superconductors*, edited by A. Furrer (Kluwer, Dordrecht, The Netherlands, 1998)

[5] M. Bosch, W. van Saarloos, J. Zaanen, cond-mat/0003236

[6] P. Monceau, F. Ya. Nad, S. Brazovskii, cond-mat/0012237

[7] S. Brazovskii, Sov. Phys. JETP **51** (1980) 342

[8] V. L. Pokrovsky, A. L. Talapov & P. Bak in *Solitons*, Edited by S.E. Trullinger, V.E. Zakharov and V.L. Pokrovsky, Elsevier Science Publishers B.V., 1986.

[9] S. Brazovskii and N. Kirova, Soviet Scientific Reviews, Sec. A, Phys. Rev., I. M. Khalatnikov Ed., vol 5, p 99 (Harwood Acad. Publ. 1984)

[10] J. H. Schon, S. Berg, Ch. Kloc, B. Batlogg, *Science*, **287**, (2000) 1022
[11] A. J. Heeger, S. Kivelson and J. R. Schrieffer, Rev. Mod. Phys. **60** (1988) 781
[12] H. Takayama, Y.R. Lin-Liu and K. Maki, Phys. Rev. B **21** (1980) 2388
[13] T. Bohr and S. Brazovskii, J. Phys. C **16** (1983) 1189
[14] G. Forgacs & al., Phase Trans. and Critical Phenom., C. Domb & J.L. Lebowitz, Vol. 14
[15] L. Bonsall and A. A. Maradudin, Phys. Rev. B, **15** (1977) 1959
[16] N. Gronbech-Jensen et al, Molec. Phys. **92**, 941 (1997)
[17] J. Leckner, Physica (Amsterdam) **176A**, 485 (1991)